DOI: 10.1002/cphc.200900950

Intermediates in the Catalytic Cycle of [NiFe] Hydrogenase: Functional Spectroscopy of the Active Site

Maria-Eirini Pandelia, Hideaki Ogata, and Wolfgang Lubitz*[a]

The [NiFe] hydrogenase from the anaerobic sulphate reducing bacterium *Desulfovibrio vulgaris* Miyazaki F is an excellent model for constructing a mechanism for the function of the so-called 'oxygen-sensitive' hydrogenases. The present review focuses on spectroscopic investigations of the active site intermediates playing a role in the activation/deactivation and catalytic cycle of this enzyme as well as in the inhibition by carbon monoxide or molecular oxygen and the light-sensitivity of the hydrogenase. The methods employed include magnetic resonance and vibrational (FTIR) techniques combined with electrochemistry that deliver information about details of the geometrical and electronic structure of the intermediates and their redox behaviour. Based on these data a mechanistic scheme is developed.

1. Introduction to [NiFe] Hydrogenases

Hydrogen conversion by the enzyme hydrogenase has become a field of intensive research in recent years due to a continuously increasing interest into attaining hydrogen-based energy sources.[1–3] Hydrogenases[4] are involved in the metabolic machinery of a wide variety of microorganisms by catalysing the reversible heterolytic splitting of dihydrogen according to the elementary reaction (1):[5]

$$H_2 \rightleftharpoons H^- + H^+ \rightleftharpoons 2H^+ + 2e^- \quad (1)$$

The production and engineering of hydrogenases is pivotal for the design of biocatalysts that are focused either on biohydrogen generation or on the biofuel cell/biosensors concept.[3,6–9]

On the basis of the metal content of their active site hydrogenases can be classified into three distinct categories: [NiFe], [FeFe] and Hmd or [Fe] hydrogenases.[10–13] The present work is focused on the study of the [NiFe] class and in particular on the hydrogenases derived from sulphate reducing bacteria, with the *Desulfovibrio (D.) vulgaris* str. Miyazaki F (MF)[14] serving as a selected representative. *D. vulgaris* MF is a δ-proteobacterium with its complete genome sequenced. It is a strict anaerobe that gains energy for growth from the reduction of sulphate to sulphide.[15] The [NiFe] hydrogenase involved in this anaerobic respiration is a periplasmic enzyme attached to the membrane with a tetrahaem cyt *c* module as its physiological electron acceptor.[16,17] It has a molecular weight of approximately 90 kDa and consists of two subunits;[18] the large subunit contains the hetero-bimetallic [NiFe] centre (known as the active site) and the small subunit contains three almost linearly arranged iron-sulphur cofactors, one [Fe_3S_4] cluster in-between two low-potential [Fe_4S_4] clusters, that are involved in the electron transfer from and to the active site[19] (Figure 1). Proton transfer involves several possible pathways. The electron and proton transfer pathways as well as the hydrophobic gas channel are indicated with arrows in Figure 1.[20–22]

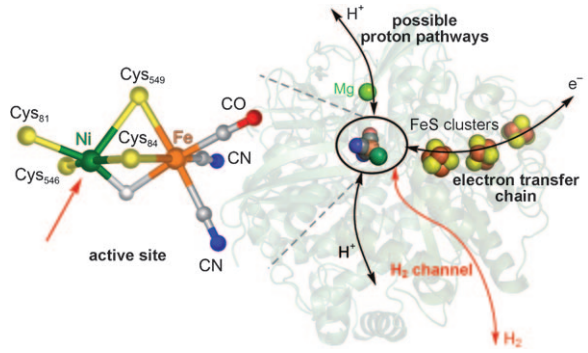

Figure 1. The active site and the iron-sulphur clusters of the [NiFe] hydrogenase from *D. vulgaris* Miyazaki F, embedded in the three-dimensional crystal structure (PDB code 1WUJ), with the protein background illustrated as a transparent ribbon. The electron transfer chain, the hydrophobic (H_2) channel and the possible proton transfer pathways are indicated by arrows. Colour code used: Ni (green), Fe (orange), Mg (light green), C (grey), O (red), N (blue), and S (yellow). The [NiFe] active site has been enlarged and shown on the left side. The vacant coordination at the Ni ion is indicated by a red arrow; the additional bridging ligand (in white colour) is not further specified (see text).

The first crystal structures of [NiFe] hydrogenases were obtained in 1995 for the *D. gigas* enzyme[23] and in 1997 for *D. vulgaris* MF, with an improved resolution for the latter.[18] The three-dimensional structure of the enzyme and its active site are shown in Figure 1. The nickel and iron metal ions are bridged by two cysteinyl residues; a third bridging ligand can be present depending on the redox state of the enzyme. Fe is additionally coordinated by three non-protein diatomic ligands, one carbonyl and two cyanides,[24,25] and it retains a low

[a] *Dr. M.-E. Pandelia, Dr. H. Ogata, Prof. Dr. W. Lubitz*
Max-Planck Institut für Bioanorganische Chemie
Stiftstrasse 34-36, 45470, Mülheim an der Ruhr (Germany)
Fax: (+49) 208-306-3955
E-mail: lubitz@mpi-muelheim.mpg.de

Supporting information for this article is available on the WWW under http://dx.doi.org/10.1002/cphc.200900950.

spin and low oxidation state ($S=0$, Fe^{2+}) in all intermediates.[26,27] The physiological origin of the CN^- ligands has been elucidated,[28] while the origin of CO still remains unclear. The nickel ion is further coordinated by two additional cysteinyl residues in a terminal fashion. Heterolytic splitting of dihydrogen is proposed to take place at the redox active nickel ion. In Figure 1, the open coordination site at the Ni opposite to the apical Cys549 is indicated, which is available for contact with substrate or inhibitor molecules. This is the position where the inhibitor CO binds[29] and the hydrophobic channels end. These channels were mapped out by Xe diffusion X-ray crystallographic experiments in the *D. desulfuricans*[30] and *D. vulgaris* MF hydrogenases.[31]

The [NiFe] hydrogenase from *D. vulgaris* MF belongs to the group of the so-called oxygen-sensitive hydrogenases.[32] In the present minireview it has been chosen as a representative example. Its structure has been determined to very high resolution in the oxidised,[18] the reduced[33] and the CO-inhibited states,[29] which have recently been reviewed.[31] Its redox chemistry consists of several intermediates that are involved in the enzyme's activation/inactivation, inhibition, light-sensitivity and in the actual catalytic cycle. Additional information on these states necessary for understanding the mechanism is available from spectroscopy. Here the focus will be on the characterization of the catalytic centre rather than the electron and proton transport chains. The paramagnetic states are studied by EPR techniques yielding detailed information about the electronic and also the geometrical structure.[11] Both EPR-active and -inactive states are amenable to infrared spectroscopy, in which the CO and CN^- ligands at the Fe serve as structural probes.[24,25] The combination with electrochemical techniques allows the pH-dependent determination of the redox transitions. Together with quantum-chemical calculations these and other techniques, like Mössbauer[34] or XAS[35,36] spectroscopies, are helpful in elucidating the details of the reaction mechanism for the [NiFe] hydrogenases.[32,37–39] The aim of this minireview is to give an overview of the current knowledge of this metalloenzyme, relate it to other species and outline the advantages and problems for the potential use of hydrogenases in future energy technologies.

2. Spectroscopic Characterisation of the Active Site Intermediates

2.1. Structure and Electronic Properties of Oxidised States: Ni-A and Ni-B

The paramagnetic oxidised states of the enzyme are called Ni-A and Ni-B. They differ in their time of reactivation under hydrogen and/or reducing conditions; Ni-B (ready) can be activated within seconds, whereas Ni-A (unready) requires prolonged activation times.[40,41] Many recent investigations are centred on the spectroscopic and chemical differences between these states with the purpose to elucidate the origin of their different properties. This is crucial in view of their distinctly different reactivation kinetics[40,42] and of recent observations that in oxygen-tolerant hydrogenases the Ni-A state is absent.[43,44,154] The determination of the exact chemical nature of the [NiFe] centre in the oxidised states in the *D. vulgaris* MF hydrogenase would therefore contribute greatly to an understanding of the oxygen inhibition in these enzymes.

The EPR spectra of Ni-A and Ni-B are characterised by rhombic g-tensors with g-values: 2.32, 2.24, 2.01 and 2.33, 2.16, 2.01, respectively[45] (see Figure 2 for an overview of the EPR spectra in *D. vulgaris* MF and Table S1 for g values). The g_z principal component is close to the free-electron g_e value, while the two other components are larger than g_e, which is typical for a Ni^{3+} with the unpaired electron ($S=1/2$) in the d_{z^2} orbital.[46] Single crystal EPR studies have shown that the direction of the z principal axis of the g-tensor in the oxidised states is parallel to the direction of the bond between nickel and the axial cysteine sulphur, which points from nickel to the vacant axial coordination position (cf. Figure 1).[47,48] The other g tensor directions could also be determined. These data were important for comparison with DFT calculations on active site models of the hydrogenase and thus instrumental in the determination of the structure and orbital distribution of these species.[49] EPR spectra of ^{61}Ni-substituted samples in the oxidised states showed that the major part of the unpaired spin density is indeed localised at the Ni ion.[50–52] ELDOR-detected NMR (EDNMR) studies on the Ni-B state of *D. vulgaris* MF allowed the determination of the complete ^{61}Ni hfc tensor. On the basis of a second-order crystal field theory approximation a spin population of 0.44 at ^{61}Ni was estimated.[53] The rest of the spin density is distributed over the nickel ligands, in partic-

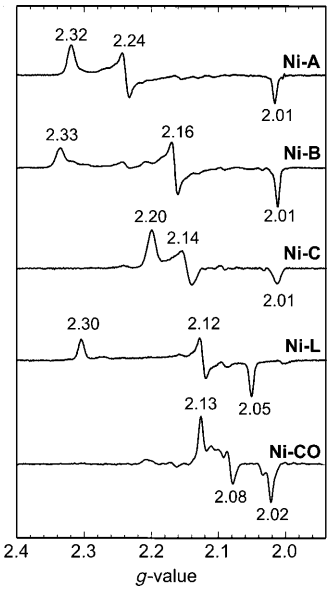

Figure 2. CW EPR spectra (X-band) of the paramagnetic states of the anaerobic [NiFe] hydrogenase from *D. vulgaris* MF. The 'unready' inactive Ni-A, the 'ready' active Ni-B state, the hydride carrying Ni-C state, the light-induced Ni-L state (Ni-L2 according to accepted nomenclature[100,119]) and the CO-inhibited paramagnetic Ni-CO complex are shown (refer to text for details). In the spectrum of Ni-CO, lines from an additional redox state are present, usually observed upon different treatments of the *D. vulgaris* MF enzyme. The principal g tensor components are given at the respective positions.

ular the sulphur of Cys549. In Figure 3 (top) the unpaired spin density distribution of a truncated model for the active site in the Ni-B state is shown. The spin density at the nickel is 0.52, at the sulphur of Cys549 it is 0.34 and at the Fe it is close to zero (0.002).[54]

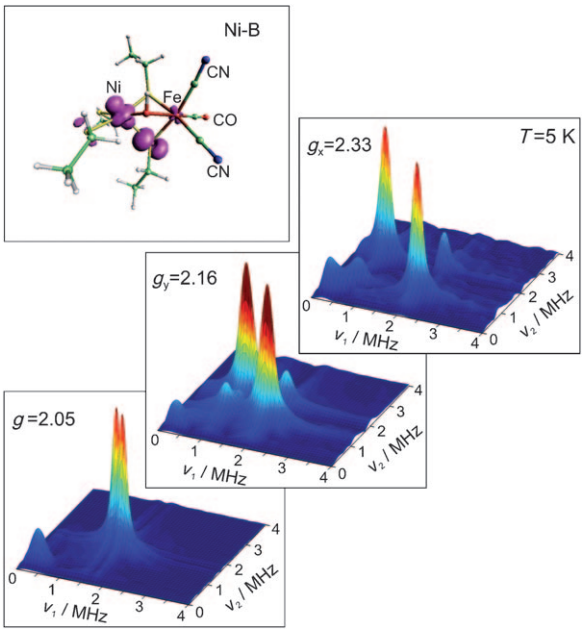

Figure 3. ^{57}Fe HYSCORE spectra of *D. vulgaris* Miyazaki F hydrogenase in the Ni-B redox state recorded at the g_x and g_y canonical orientations and at $g=2.05$ (Ogata et al. to be published). Experimental conditions: Q-band frequency (~34 GHz), $\tau=336$ ns, 256×256 data points, 5 K. (Top) DFT calculation: Contour plot of the unpaired spin density distribution (0.005 e/a_0^3) of a truncated model of the active site in the Ni-B state (OH^- bridge). In the oxidised ready Ni-B the spin density at the Ni is 0.52, at the axial sulphur of Cys549 it is 0.34, at the terminal sulphur Cys546 it is 0.06 and 0.002 at the Fe, resulting in a very small ^{57}Fe hyperfine interaction.[49]

That the Fe ion is diamagnetic (Fe^{2+} low spin, $S=0$) has already been concluded earlier based on EPR and Mössbauer spectroscopy on hydrogenases from other species,[55,56] as well as Q-band ENDOR measurements on ^{57}Fe substituted samples from *D. gigas*[55,57] and *D. desulfuricans*. To precisely determine the spin delocalisation at the Fe, a series of ^{57}Fe HYSCORE experiments were performed (Ogata et al., to be published). In Figure 3 spectra for the Ni-B redox state recorded at the g_x and g_y canonical orientations and at $g=2.05$ are shown as an example. The ^{57}Fe hyperfine tensor is rhombic with the largest component being $A_x=1.4\pm0.2$ MHz; the isotropic hyperfine coupling constant is 0.8 ± 0.2 MHz. The tensor magnitude is very similar to that reported previously for *D. gigas* for Ni-A[55] and consistent with the density functional calculations.[54]

X-ray crystallographic experiments on the oxidised enzyme detected additional electron density in the bridging position between the two metals. EPR experiments with $^{17}O_2$-labelled gas[58] and $H_2{}^{17}O$-enriched water[59] have shown that an oxygen species is present in the active site of both oxidised states that can be derived either from the gas or the solvent water.

These experiments revealed for Ni-B the presence of a mono-oxo bridge between the two metal ions (Ni-Fe distance 2.7 Å), however its exact chemical identity could not be elucidated. Analysis of the EPR line shape for the Ni-B state in H_2O/D_2O exchange experiments showed the presence of an exchangeable proton in the vicinity of the spin carrying Ni-Fe centre.[60] Single crystal ENDOR and HYSCORE studies performed on this (H/D) exchangeable proton in the *D. vulgaris* MF hydrogenase led to the determination of the hyperfine tensor and, together with DFT model calculations, to a determination of the position of this acidic proton.[61,62] This identified the oxygenic ligand in Ni-B as a hydroxide (μ-OH^-) bridging the Ni and the Fe.

In the case of the Ni-A state,[63] the two metal centres Ni-Fe are found in a slightly longer distance (2.8 Å) compared to Ni-B. Up to date, the chemical identity of the oxo-based ligand in Ni-A could not be determined with confidence. X-ray structural studies of the Ni-A state in *D. fructosovorans* ,[64] and in *D. vulgaris* MF[63] have postulated a di-oxo or an SO species. On the other hand, theoretical calculations support either a monoatomic oxygenic species similar to Ni-B or a hydroperoxide.[61,65,66] Interestingly, in addition to a different bridging ligand, both experimental and theoretical approaches consider the possibility of sulfoxides (S=O) or sulfenic acids (SOH)[42,63,67] as a plausible origin for the differences between Ni-A and Ni-B.[63,66,68] In support of the latter, studies with Ni thiolate compounds have resulted in S-oxidation products upon reaction with O_2,[69] though their formation in most of the cases is irreversible[70–72] or reversible only at very negative potentials requiring a two-electron reduction.[73]

Previous investigations of the oxidised states in H_2O/D_2O prepared samples from the *A. vinosum* hydrogenase, showed the presence of an exchangeable proton in the vicinity of the [NiFe] site only for the Ni-B state.[60] However, HYSCORE experiments on the *D. vulgaris* MF demonstrated the presence of an (H/D) exchangeable ligand also in the active site of Ni-A.[61] This could be observed only after reductive activation with D_2 in a D_2O-based buffer followed by a subsequent reoxidation to the Ni-A state. On the basis of this observation, the presence of a non-protonated O^{2-} or SO molecule as bridging ligand was excluded. The results show that there is an exchangeable proton associated with the bridging ligand that in contrast to Ni-B is not solvent accessible. In addition, a difference between the magnitude of the hyperfine coupling corresponding to this proton between Ni-A and Ni-B states was observed.

ENDOR experiments have been carried out on the Ni-A state in single crystals of *D. vulgaris* MF hydrogenase in order to elucidate the identity of the bridging ligand in Ni-A (Ogata et al to be published), similar to previous experiments performed on Ni-B.[62] Figure 4 shows ENDOR spectra of the Ni-A state at a specific orientation of the single crystal with respect to the magnetic field in both protonated and deuterated single crystals. In the deuterated Ni-A state one ^{1}H hyperfine coupling is absent (indicated by the dashed lines) that is assigned to the exchangeable proton of the bridging ligand. The ENDOR spectra were analysed as has been previously described by using the knowledge of the g tensor orientation with respect to the

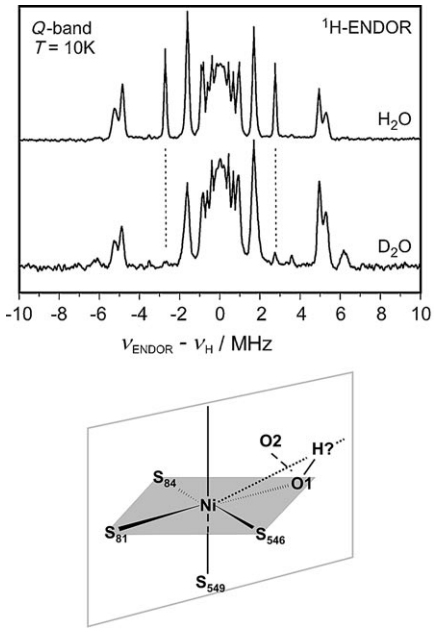

Figure 4. Q-band single crystal Davies ENDOR spectra of a sample in the Ni-A state of the *D. vulgaris* Miyazaki F [NiFe] hydrogenase prepared in H_2O (D_2O)-based Tris buffer, subsequently reduced by H_2 (D_2) and then reoxidised using a protonated (deuterated) Na_2S-containing buffer, respectively.[63] These traces are taken from a series of spectra with rotation of the crystal around the crystallographic *c*-axis in the *ab* plane. Upon (H/D) exchange a proton hyperfine coupling clearly disappeared as indicated by the black dotted line. The magnitude and the orientation dependence of the hyperfine tensor showed that this nucleus is in the vicinity of the spin carrying [NiFe] centre. Its possible location in the [NiFe] complex is shown in the lower part of this figure (Ogata et al. to be published).

crystallographic axes.[47,48] The analysis of the angular dependence of the hyperfine coupling gave, together with DFT calculations, a position of this exchangeable proton near the spin carrying [NiFe] site that is depicted in Figure 4 (bottom). The position of the proton and the calculated hyperfine couplings of the bridging ^{17}O and ^{1}H are in closer agreement with a bridging hydroxyl than with a hydroperoxide for Ni-A (Ogata et al., to be published). The orientation of the proton in the hydroxide of Ni-A is different from that in the Ni-B state.[61]

In the as-isolated, oxidised enzyme from *D. vulgaris* MF the active site is found in a mixture of the Ni-A and Ni-B states. The iron-sulphur clusters are then in their most oxidised forms; $[Fe_3S_4]^{1+}$ ($S=1/2$) and $[Fe_4S_4]^{2+}$ ($S=0$).[74,75] At low temperatures the EPR spectrum of the $[Fe_3S_4]^{1+}$ cluster can be observed. Similar electronic characteristics for this centre have been obtained in *D. gigas* and *D. vulgaris* MF hydrogenases.[76] By W-band EPR, the *g*-tensor of the $[Fe_3S_4]^{1+}$ in *D. vulgaris* MF was measured (2.0257, 2.0174, 2.0114)[77] and by Mössbauer spectroscopy in *D. gigas* the inner electronic structure of the $[Fe_3S_4]^{1+}$ as well as the spin projection factors of the three Fe ions were determined.[78]

A direct interaction between the [NiFe] site in the Ni-A/B states and the $[Fe_3S_4]^{1+}$ is not observed in the EPR spectra since the distance is too large (i.e. 2.1 nm). This can, however, be measured by pulsed ELDOR (electron-electron double resonance), as has recently been shown for *D. vulgaris* MF.[79] The experiment measures the dipolar coupling between the paramagnetic [NiFe] and $[Fe_3S_4]^{1+}$ centres from which distance and orientation can, in principle, be obtained; this information can then be related to the crystal structure. The four-pulse ELDOR time trace spectrum of the *D. vulgaris* MF hydrogenase in the Ni-A state is shown is Figure 5. Using the point-dipole approxi-

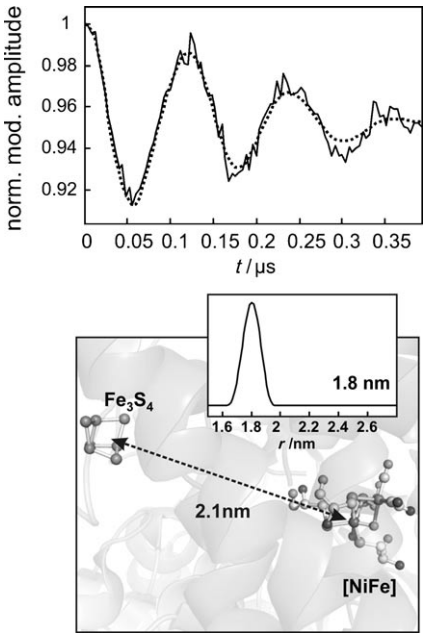

Figure 5. Baseline-corrected time trace obtained by a dead-time free four-pulse ELDOR experiment performed on the oxidised state Ni-A of the [NiFe] hydrogenase from *D. vulgaris* Miyazaki F (top). The dotted trace corresponds to a simulation obtained either by the approximate Pake transformation (APT) or the Tikhonov regularization. The experiment aims at the determination of the dipolar interaction between the two spin-carrying centres, namely the [NiFe] site and the medial $[Fe_3S_4]^{1+}$ cluster (only these two metal centres are illustrated—the in-between $[Fe_4S_4]$ is not shown). The distance distribution (shown in the inset) was estimated from the frequency of the dipolar interaction is 1.80 nm ($\pm$0.07). The average distance between the Ni centre that carries the majority of the spin and the 'centre' of the $[Fe_3S_4]^{1+}$ is 2.1 nm (PDB code 1WUJ) (bottom). Experimental conditions: $B=3420$ G with $\nu_{det}=9.775$ GHz ($g_{det}=2.043$) and $\nu_{inv}=9.674$ GHz ($g_{inv}=2.022$), $T=5$ K (Pandelia, unpublished data).

mation, the measured frequency of 8.2 MHz, corresponds to a distance of 1.80 nm, which is 0.3 nm shorter than the average obtained from the crystal structure.[63] This deviation shows that for a meaningful interpretation, distance measurements between multicentre metal clusters have to consider the individual spin projections and spin delocalisation of the centres involved.[79,80] ELDOR measurements in 'pure' Ni-A and Ni-B samples from the *D. vulgaris* MF hydrogenase performed in this laboratory, yielded within error identical results. Thus, it can be inferred that there is no major change in the spin distribution and the distances between the dipolar coupled paramagnetic centres in these two states.

On the basis of their FTIR frequencies the Ni-A and Ni-B states are spectroscopically also not very different (Figure 6, Table S2). Fourier transform infrared spectroscopy monitors the IR frequencies corresponding to the intrinsic CO, CN^- ligands

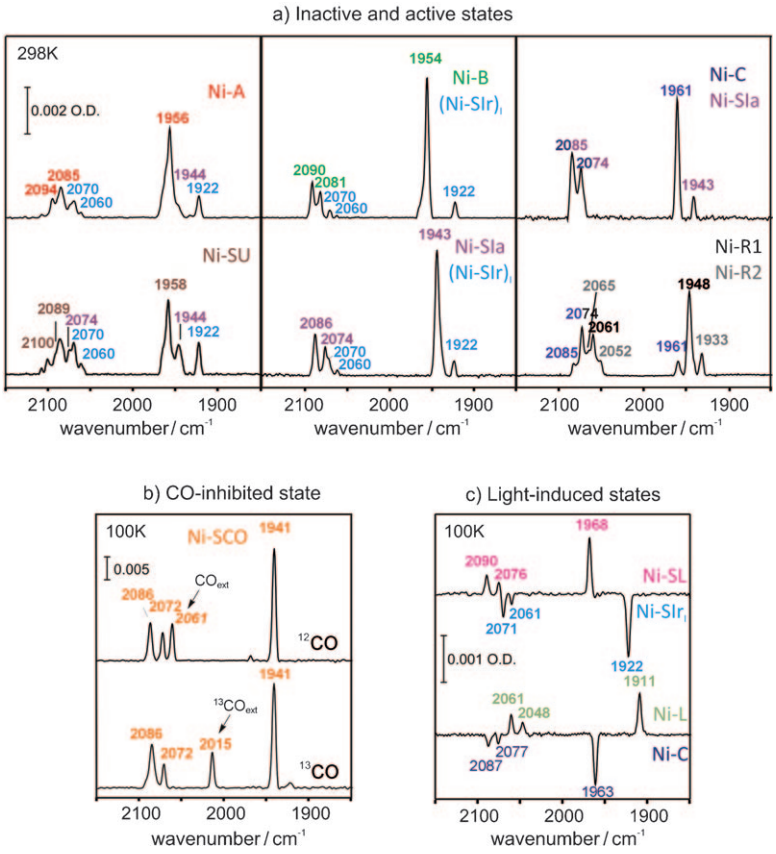

Figure 6. Overview of the FTIR spectra corresponding to all observable redox intermediate states of the anaerobic [NiFe] hydrogenase from *D. vulgaris* Miyazaki F. The states are divided according to the following subgroups; a) inactive (oxygen-inhibited) and catalytically active intermediates, b) CO-inhibited state (Ni-SCO) using ^{12}CO and ^{13}CO, and c) light-induced states. The light-sensitive intermediates are shown in light-minus-dark difference spectra that relate them directly to the respective dark educt states. Each state has been assigned a different colour for easier identification.

at the Fe that are very sensitive probes for electronic changes in the active site of hydrogenases. Each redox state is characterised by a set of three bands, one of high intensity in the range 1900–1970 cm^{-1} corresponding to the π-back bonded CO and two less intense in the range 2040–2100 cm^{-1} corresponding to the vibrationally coupled CN^- ligands. An overview of the FTIR spectra of the various states of the [NiFe] hydrogenase of *D. vulgaris* MF is given in Figure 6. The CO and CN^- stretching vibrations corresponding to the Ni-A and Ni-B states are very similar, which shows for both states a similar electron density delocalisation at the Fe, and consequently at the [NiFe] site.

2.2. The One-Electron Reduced EPR-Silent States

Upon one-electron reduction of Ni-A and Ni-B, the Ni-SU and Ni-SI$_r$ intermediates are respectively formed, while the medial cluster is reduced to $[Fe_3S_4]^0$. Ni-SU and Ni-SI$_r$ are EPR-silent and catalytically inactive,[41,81,82] but have distinct FTIR spectroscopic signatures allowing their identification (Figure 6). The Ni-SI$_r$ ('silent ready') state exists in two isoelectronic acid-base forms, (Ni-SI$_r$)$_I$ and (Ni-SI$_r$)$_{II}$, for which to date no solid structural information exists. On the basis of different spectroscopic findings from FTIR electrochemical measurements two possibilities have been postulated for the Ni-SI$_r$ intermediates. In the case of *A. vinosum*, the (Ni-SI$_r$)$_I$ is proposed to retain the OH^- ligand from Ni-B and the more protonated (Ni-SI$_r$)$_{II}$ is suggested to have a H_2O loosely coordinated to its active site.[81] For the *D. gigas* and *D. fructosovorans* enzymes, however, experiments have lead to the conclusion that (Ni-SI$_r$)$_I$ carries no μ-oxo species, while (Ni-SI$_r$)$_{II}$ differs by the degree of protonation of one of the coordinating sulphurs.[83]

A very recent investigation on the *D. vulgaris* MF hydrogenase contributed to understanding the structure of this state.[84] In that work, the (Ni-SI$_r$)$_I$ state was shown to be light-sensitive at cryogenic temperatures, leading to formation of a novel state Ni-SL (see Figure 6). This photoinduced transition is reversible. Temperature dependent kinetics of the back conversion from Ni-SL to (Ni-SI$_r$)$_I$ and a small (H/D) kinetic isotope effect led to the conclusion that the structural changes upon illumination are related to the bridging OH^- ligand. This suggests that the ligand remains still bound to the active site of (Ni-SI$_r$)$_I$. Wavelength dependence of the photoconversion revealed that light induces a nickel centred electronic transition that triggers rearrangement of this oxygenic ligand. Displacement of the latter is feasible in (Ni-SI$_r$)$_I$ and not in Ni-B due to its weaker bond with the divalent nickel ion (Ni^{2+}). The present results on *D. vulgaris* MF are in agreement with the scheme proposed for enzyme activation in *A. vinosum*[81] and related oxygen-sensitive hydrogenases from sulphate reducing bacteria[12] and is supported by relativistic DFT studies on intermediates states of [NiFe] enzymes.[85]

One-electron reduction of Ni-A produces the Ni-SU ('silent unready') state. It has been proposed that the rate-limiting step during the activation process from 'unready' hydrogenase molecules is the first-order conversion of Ni-SU to the Ni-SI states.[86] Ni-A has been shown not to react directly with H_2 and a reductive step to Ni-SU is a prerequisite for the enzyme to interact with hydrogen.[70] The transition to Ni-SU is reversible at 2 °C, while this is not the case for the inactive ready states (oxidation from Ni-SI$_r$ to Ni-B).[81] The FTIR spectrum of Ni-SU has bands at slightly higher frequencies compared to the Ni-A state. This is opposite to what is observed for the reduction of Ni-B to Ni-SI$_r$ indicating a different character of the

respective electronic transitions. Up to present, the only exception was the *D. vulgaris* MF enzyme.[87] However, it was recently shown that the FTIR spectrum of Ni-SU in *D. vulgaris* MF is similar to the ones reported in other standard hydrogenases (Figure 6). The midpoint reduction potential at pH 8.2 was found to be −278 mV,[88] in very good agreement with EPR redox titrations for the reduction of Ni-A in *D. vulgaris* MF.[76]

These one-electron transitions to the EPR-silent states are coupled to proton transfer. A possible protonation of one of the coordinating sulphurs has been thus postulated as crystal structures have shown a high temperature factor for the terminal Cys546[29] that is located close to the suggested proton transfer pathway[20,83] (Figure 1). This cysteine is replaced by a selenocysteine in the subgroup of [NiFeSe] hydrogenases.[89,90]

After reactivation the oxygenic species is no longer bound to the active site and a transition to the Ni-SI_a state occurs. The (Ni-SI_r)$_{II}$ and Ni-SI_a states have been reported to have within the spectral resolution identical FTIR spectra in the case of *A. vinosum*,[41,81] whereas for other oxygen-sensitive enzymes only the active Ni-SI_a (or Ni-SI_{II} according to some authors) is proposed.[91–93]

Regarding the spin state of the divalent nickel ion, only a high-spin Ni^{2+} species with a distorted tetrahedral geometry is in agreement with the one-electron reduced Ni-$SI_{r/a}$ states according to calculations[37,94] considering a four-coordinated nickel centre. This is further supported by Ni L-edge X-ray circular magnetic dichroism (XCMD) measurements on *D. desulfuricans* and *D. gigas*.[95] However, there are studies that have reproduced the experimental FTIR frequencies considering a low-spin ($S=0$) nickel centre;[96,97] high level ab initio calculations also predict a singlet state for the Ni-$SI_{r/a}$ states rather than a triplet.[98] Theoretical results are very dependent on the computed ground state and the functionals applied, thus no unique answer has been obtained so far regarding the actual spin state of these EPR-silent states. All models, however, are in agreement with an elongated Ni-Fe distance of 2.8 Å or greater for this state, which is significantly longer than the one found for the most reduced EPR-silent state, Ni-R, as discussed below.

2.3. The Catalytic Intermediate Ni-C

Further reduction of the hydrogenase molecules in the Ni-SI_a state, yields the paramagnetic catalytic Ni-C intermediate. The crystal structure of the reduced enzyme from *D. vulgaris* MF (probably a mixture of Ni-C/Ni-R) did not show any additional electron density at the position of the third bridging ligand;[99] the two metals are now in a closer distance of 2.6 Å.

The EPR spectrum of Ni-C in *D. vulgaris* MF ($g=2.20$, 2.14, and 2.01) is very similar to that of all other [NiFe] hydrogenases studied so far (Figure 2). It exhibits a smaller *g*-anisotropy compared to the spectrum of the Ni-A/Ni-B states, but the g_z principal component remains close to the free electron g_e value indicating a Ni^{3+} d_{z^2} ground state. Single crystal EPR studies on *D. vulgaris* MF have shown that the g_z component points towards the empty coordination site, indicating that the bridging position in the equatorial plane of the molecule is occupied, similarly to the Ni-A/B states.[100] Pulsed EPR spectroscopy using (H/D) isotope labelled reduced samples contributed greatly to the identification of this ligand. Ni-C in *D. gigas* was shown to be accessible to solvent exchange in D_2O and ESEEM measurements showed ^2H hyperfine couplings indicative of a hydron in close proximity to the metal ion.[101] H/D exchangeable ENDOR signals in the Ni-C state of *D. gigas* and *D. baculatum* provided further evidence for a hydron binding in this state;[57,102,103] theoretical calculations predicted the binding of a hydride.[96,104,105]

^1H and ^2H HYSCORE and ENDOR experiments first on the regulatory hydrogenase from *Ralstonia* (*R.*) *eutropha*[106] and later on *D. vulgaris* MF[107] using H/D exchange, uniquely identified a hydride ligand (H^-, D^-) in the bridging position between Ni and Fe. Its location was estimated from the analysis of the hyperfine tensor and a point-dipole approximation, in good agreement with DFT calculations on geometry optimised models of Ni-C.[105] It is important to mention that the ^2H Q-band ENDOR study on *D. gigas*[57] showed the presence of two types of exchangeable protons in the Ni-C state; one exchangeable proton that has a large hyperfine coupling and corresponds to the hydride ligand and a second smaller coupling. The second coupling was proposed to correspond to a water molecule near the active site. A final conclusion on the assignment of this proton remains to be elucidated in view of proposed structural schemes of Ni-C involving more than one hydrogenic species in the active site.[92,108]

EPR spectra of Ni-C at low temperatures (below 20 K) for the *A. vinosum, D. gigas* and *D. vulgaris* MF hydrogenases show complex ("split") signals reminiscent of a magnetic interaction between the [NiFe] site and the proximal [Fe_4S_4] cluster that has become reduced to the paramagnetic [Fe_4S_4]$^{1+}$ state.[74,76] This spin–spin interaction has been studied in detail for the *D. gigas* hydrogenase[109] and has also been detected for *D. vulgaris* MF[51] and *A. ferrooxidans*[110] hydrogenases. Information about the exchange interaction (*J*) as well as estimates of the distances and relative orientations of the spin centres could be obtained.[109] Furthermore, the reduction potentials of the two [Fe_4S_4] clusters have been estimated for *D. gigas*, *A. vinosum* and *D. vulgaris*; they are lower than −300 mV.[75,76,111] These clusters have been spectroscopically distinguished by Mössbauer spectroscopy.[75] The distal cluster (close to the surface, see Figure 1) has a slightly more negative redox potential with a value near to the one of the low-potential physiological acceptor cytochrome c_3.[17]

The FTIR spectrum of Ni-C in *D. vulgaris* MF is described by a high CO stretching frequency at 1961 cm^{-1}, while the coupled CN^- vibrations are quite similar to those of Ni-SI_a (Figure 6, Table S2 in the Supporting Information). The FTIR frequencies and their shifts directly reflect changes in the valence state and coordination environment of the Ni centre.[112] The influence of redox and protonation state of the [NiFe] active centre on the length of the CO bond has been modelled by predicting the CO bond distances as a function of the redox and protonation state.[96] In the case of Ni-C the observed shift towards higher frequencies indicates a shorter CO bond (lower electron density at the Fe).

In addition, a change in the protonation state of one of the coordinating sulphurs has been inferred by the varying calculated atomic charges of these ligands and different Ni-sulphur distances,[113] in agreement with X-ray crystallographic results.[99] A possible involvement of the terminal cysteine Cys546 in the heterolytic cleavage of molecular hydrogen has thus been postulated by a protonation of this sulphur ligand in Ni-C.[105,113]

2.4. The Fully Reduced State(s) Ni-R

The most reduced state of the enzyme is Ni-R and is reached by one-electron reduction of Ni-C. The FTIR spectrum of the Ni-R state in *D. vulgaris* MF, as well as in other standard hydrogenases, is a mixture of two or more isoelectronic forms that differ in their degree of protonation[91] (see Figure 6). The electronic transition from Ni-C to Ni-R is accompanied by a small increase of the electron density at the Fe, in agreement with the lowering of the stretching frequencies observed by IR spectroscopy. During catalytic turnover, Ni-C is the only state in equilibrium with Ni-R,[41,82,114] suggesting that the hydride remains present also in this state.[32,39,85,92] Ni-R is EPR-silent with a divalent nickel proposed by theoretical calculations to be in a high spin state (Ni^{2+}, $S=1$). All geometry optimised models are in line with a hydride bridge and a Ni-Fe distance of 2.6 Å, fully compatible with X-ray data on *D. vulgaris* MF and *D. baculatum*.[90,99]

Ni-R can exist in up to three different protonation states, while several transition states have been proposed in order to account for a heterolytic splitting of dihydrogen. In this context, an ONIOM theoretical study suggested the possibility of a Ni^{1+} species that can bind two hydrides leading to Ni^{3+} and then results in a Ni^{2+} with a hydride bridge for Ni-R.[115] More recently, a series of possible structural models for the different Ni-R forms of the *D. vulgaris* MF has been constructed on the basis of a comparison with synthetic Ni-Ru complexes that can perform heterolytic splitting of H_2.[31,116,117] In all possible forms of Ni-R the presence of one or more hydrides is suggested; this provides a stable coordination environment for the Ni ion in all the catalytic intermediates that involves minimal conformational changes, thus allowing for the very rapid catalytic turnover of the enzyme observed.[92]

3. Light-Induced Structural Changes in the Active Site

Among the inactive oxidised states of the enzyme, the $(Ni\text{-}SI_r)_I$ state from *D. vulgaris* MF has recently been shown to be light-sensitive,[84] (see Figure 6c and discussion above). The photoinduced process has been related to the displacement of the oxygen-based ligand (OH^-) from the active site in this state, facilitated by the reduction of the nickel ion to Ni^{2+}. These experimental results have strengthened structural schemes for the enzyme that support an oxo-bound species in the $(Ni\text{-}SI_r)_I$ state.[11,12,81] It should be mentioned here, that Ni-A but not Ni-B, has been demonstrated to be light-sensitive, but the yield of the photoconversion product is substoichiometric (i.e. 5% of the Ni-A amount)[84] under the same conditions of illumination. The structural change in this case remains unclear.

The light sensitivity of the Ni-C species at cryogenic temperatures is a common feature of all [NiFe] hydrogenases. The photoconversion of Ni-C to a paramagnetic state, termed Ni-L, was spectroscopically identified by EPR first in *A. vinosum*[118] and later for several other hydrogenases.[107,119,120] This process has been associated with the light-induced loss of the hydride bridge, as shown by the disappearance of the signals corresponding to this (H/D) exchangeable ligand in the HYSCORE spectra.[106,107] Up to three light-induced Ni-L states have been identified, depending on the origin of the enzyme, and the duration and temperature at which the illumination was performed.[106,120,121] The EPR spectrum of Ni-L in *D. vulgaris* MF hydrogenase is characterised by a rhombic *g*-tensor with principal values of 2.30, 2.12, 2.05[107] (Figure 2). The electronic properties of Ni-L are different from those of Ni-C; in particular, the smallest *g* tensor component g_z is shifted from 2.01 to 2.05. This has prompted the suggestion that Ni-L is a formal Ni^{1+} centre, even though analysis of Ni L-edge XAS spectra reveal no significant change in the oxidation state of the nickel ion.[122] DFT calculations of Ni-L models support a formal Ni^{1+} with a vacant bridge, proposing that the hydride is lost upon illumination as a proton that is transferred to a nearby base.[105] A more detailed analysis of the electronic structure of Ni-L shows that this species is best described by a mixed $d_{z^2}/d_{x^2-y^2}$ ground state.[123]

FTIR spectroscopy has shown that upon illumination the bands corresponding to the Ni-C state disappear and are replaced by stretching vibrations of Ni-L at lower frequencies. A light-minus-dark FTIR difference spectrum for the *D. vulgaris* MF hydrogenase is shown in Figure 6c. Rapid scan kinetic measurements (Figure 7a) showed that rebinding of the hydride ligand as a proton is a first-order process.[124] The determined activation barrier is 46 kJ mol^{-1}. Back conversion in the dark to Ni-C was investigated by studying the rebinding kinetics of this ligand in protonated (H_2/H_2O) and deuterated (D_2/D_2O) samples. The primary kinetic isotope effect on the re-association rate constants lies between 5 and 7 (Figure 7c, KIE = 5.9 at 155 K) and demonstrates that the proton transfer is the rate-limiting step during back conversion from the Ni-L to the Ni-C state.

The Ni-R state in *D. vulgaris* MF has also been shown to be light-sensitive.[125] The photo-induced transition is suggested to correspond to the displacement of a ligand bound to the active site, which on the basis of proposed structural schemes is most likely a hydride ligand.

4. Inhibition of the Enzyme by Carbon Monoxide

It has been shown that carbon monoxide inhibits the catalytic function of hydrogenase enzymes.[126,127] FTIR and EPR experiments with ^{13}CO labelled gas on *A. vinosum* as well as X-ray crystallographic studies on *D. vulgaris* MF have demonstrated that the exogenous CO ligand binds to the nickel ion in the active site.[29,58] This indicates that the nickel is indeed the site

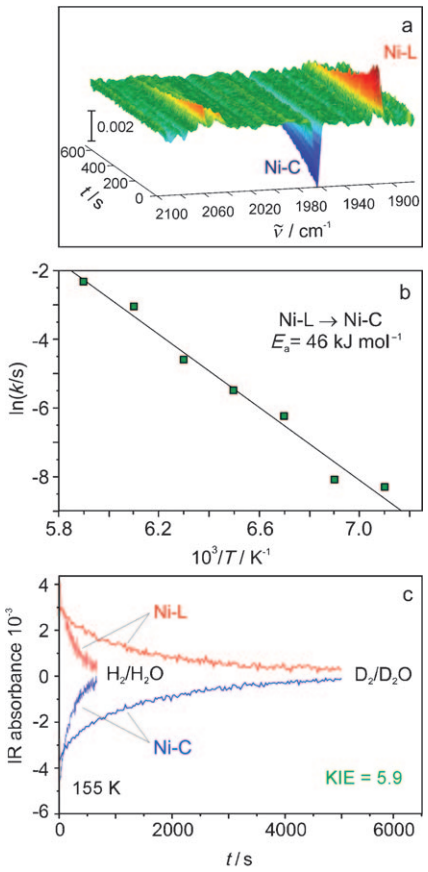

Figure 7. a) Three-dimensional presentation of the time evolution of the light-minus-dark FTIR difference spectra of the H_2 reduced hydrogenase from *D. vulgaris* Miyazaki F at 150 K after switching off the light. b) Arrhenius plot of the temperature dependence of the kinetic rates in the range between 170 and 140 K for the H_2 reduced enzyme. The activation barrier for the conversion was estimated to 46 kJ mol^{-1}. c) (H/D) kinetic isotope effect on the Ni-L to Ni-C back conversion showing the rebinding of a proton as the rate determining step. The KIE at 155 K was 5.9.[124]

of hydrogen attachment and conversion. Two electronically distinct CO-inhibited states have been observed; an EPR-silent (Ni-SCO) and a paramagnetic (Ni-CO) species. Binding of carbon monoxide to the active Ni-SI$_a$ state, results into the formation of two EPR-silent CO-bound complexes (Ni-SCO and Ni-SCO$_{red}$).[128,129] The one-electron difference between these states is attributed to the reduction of the proximal [Fe_4S_4] cluster[128,129] in the latter. In *D. vulgaris* MF as well as in *D. desulfuricans*, the extrinsic carbonyl appears in the FTIR spectra at a frequency of 2056 cm^{-1}, showing a similar weak π-back bonding to the nickel (Figure 6b).

The paramagnetic CO inhibited state can be formed by treating a solution containing Ni-C with carbon monoxide followed by illumination to generate Ni-L, in which the nickel ion is in the Ni^{1+} state (monovalent).[129,130] Based on the different rebinding kinetics during dark adaptation, binding of CO to Ni-L is favoured as compared to the insertion of the hydride. The EPR spectrum of the Ni-CO in *D. vulgaris* MF is characterised by a rhombic *g*-tensor with principal values 2.13, 2.08, 2.02 (Figure 2). These *g*-values resemble those reported previously for the *A. vinosum* and *Methanococus* (*M.*) *voltae* hydrogenases,[58,131] showing that enzymes derived from different organisms have a similar electronic structure. The experimental data could be accurately reproduced by DFT calculations considering a formal Ni^{1+} species with an axially bound CO to the nickel.[132] This accounts for the fact that Ni-CO can be generated only upon interaction with Ni-L and not with Ni-C, since binding of carbon monoxide to a Ni^{3+} is chemically unfavourable. The *g*-values of Ni-CO are significantly smaller than those of the other paramagnetic states of hydrogenase (i.e. Ni-A, Ni-B, Ni-C, Ni-L, see Table S1 in the Supporting Information). This is a consequence of the larger ligand field splitting induced by the binding of the CO to nickel. The Ni-CO converts reversibly to Ni-L upon illumination/dark adaptation.

Light-induced effects on the Ni-SCO state have been examined by FTIR experiments on *A. vinosum*[133] and X-ray crystallographic studies on *D. vulgaris* MF.[29] The Ni-SCO state is light-sensitive, leading to the photolysis of the extrinsic CO bound to the nickel. In the case of the *D. vulgaris* MF hydrogenase and at temperatures below 100 K, the Ni-SCO state converts to Ni-SI$_a$ that is identified as the only photoproduct. This is in agreement with results showing that Ni-SI$_a$ is the only physiological state of the enzyme that has the affinity for binding CO. The Ni-CO bond can be restored in the dark; the CO recombination rate constants are of bi-exponential character and the activation barrier is determined to be 9 kJ mol^{-1} approximately.[129] This lies well within the range of the energy range reported for a reversible rebinding of CO in other metalloproteins, for example, myoglobin.[134]

5. Interactions of the Active Site with the Protein Surrounding

The [NiFe] centre is bound to the polypeptide backbone by 4 cysteine residues (Figure 1), which play a major role for the structure, the electronic properties and the catalytic function of the enzyme. EPR experiments have clearly demonstrated the ability of these soft ligands to affect the spin and charge density delocalisation, thereby changing the electronic properties of the metal site. Furthermore the sulphurs can act as a "base" for the protons that are involved in the hydrogen conversion process. On the other hand, these sulphurs are also amenable to oxidation, which might be implicated in reactions with molecular oxygen. In addition to these direct ligands of the active site there are other interactions with the protein surrounding, for example, hydrogen bonds, that play a role in the geometrical stabilization and fine tuning of the electronic and catalytic properties of the [NiFe] centre. These hydrogen bonding interactions are depicted in Figure 8.

Pulsed EPR experiments on the Ni-A and Ni-C states of the *D. gigas* hydrogenase, identified signals attributable to a ^{14}N nucleus in close proximity of the active site.[101] Based on the magnitude and asymmetry of its quadrupolar interaction, this was assigned to a remote nitrogen of an imidazole group. Signals of this ^{14}N nucleus were shown to be present also in the case of the *D. vulgaris* MF enzyme[135] and were assigned to the N_ε of a histidine (His88) that coordinates the apical Cys549 and is strictly conserved in all catalytic hydrogenases (Figure 8). In

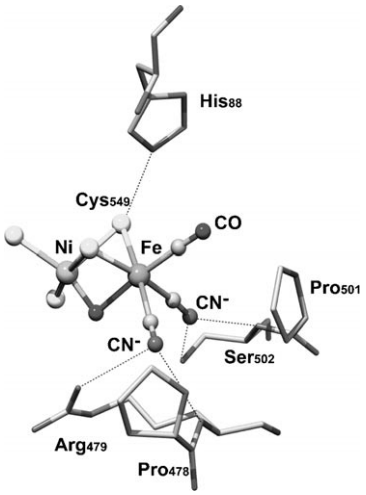

Figure 8. Three-dimensional structure of the active site of the [NiFe] hydrogenase from *D. vulgaris* Miyazaki F in the Ni-B state (PDB code 1WUJ). The putative hydrogen bonds to the direct ligands of the [NiFe] complex are represented with dotted lines.

support of this assignment, similar studies on the Ni-C state of the H_2-sensing hydrogenase from *R. eutropha*, in which this residue is replaced by a glutamate, showed no such ^{14}N signals.[136] A site-directed mutation of this glutamate to a histidine residue recovered the resonances of this ^{14}N nucleus in the ESEEM spectra, as observed in *D. gigas* and *D. vulgaris* hydrogenases.[51,101]

A more detailed pulsed EPR and HYSCORE examination fully supported the nitrogen coordination of the active site in *D. vulgaris* MF[137] by His88, using natural abundance and ^{15}N-enriched histidine samples as well as a comparison with DFT calculations. The effect of the hydrogen bond between His88 and Cys549 on the local structure of the [NiFe] active site was examined and it was shown to fine-tune its electronic properties, denoting its important role in the function and catalytic activity of the enzyme.[137]

On the basis of the crystal structures available, each of the cyanide ligands bound to the Fe can form up to two putative hydrogen bonds with nearby amino-acid residues (Figure 8). Such interactions are probably important for a fine tuning of the redox potential of the metal and the active site in general.[138] The hydrogen bonding has been experimentally demonstrated by FTIR spectroscopy on the *D. fructosovorans* hydrogenase, for which these amino-acids were mutated to residues that cannot form hydrogen bonds.[139] This resulted in shifts in the FTIR spectra only of the CN^- stretching vibrations. In addition, for the *D. vulgaris* enzyme it was shown in our laboratory that the hydrogen-bonding and/or electrostatic interactions of the active site with these neighbouring amino-acid residues can be modulated by the colour of the monochromatic light used for illumination at low temperatures (<40 K). A light-induced isomerisation has been postulated.[84] The exact reason for this 'perturbation' of the hydrogen-bonding network around the CN^- ligands is still unclear.

6. Integrating Spectroscopy and Electrochemistry:

6.1. Hydrogenases in Solution and Adsorbed on Surfaces

The widely applicable method of protein film electrochemistry (PFE) uses the adsorption of the enzyme directly onto an electrode surface that plays the role of its redox partner.[7,140] Using PFE the reaction of the *D. vulgaris* MF enzyme with sulphide (H_2S) has been examined in view of the presence of a "μ-sulfido" species previously reported for the Ni-Fe bridge.[18] It was shown that active hydrogenase adsorbed on a rotating pyrolytic graphite electrode reacts reversibly with hydrogen sulphide in a pH-dependent manner.[141] Enzyme inactivation occurs only if a hydrogen sulphide solution is injected at potentials more positive than $+100$ mV. This inactivation is most likely related with the formation of an adduct with a sulphide ligand. However, the biological relevance of such a state still remains unclear, since it is formed only at very oxidising conditions.

Cyclic voltammetry and a variety of chronoamperometric experiments can be carried out under varying conditions of temperature and gas composition (i.e. N_2, H_2, O_2, CO, etc.) with the aim to study inter-conversion between active/inactive forms, electron-transfer rates and reactions with inhibitors.[142,143] However, this method alone is not adequate to obtain structural information about the intermediates observed, since results cannot be correlated directly with spectroscopic features. In this respect, the immobilization of hydrogenases on a thin gold electrode on the surface of a silicon semicylindrical crystal offers the possibility of combining direct redox experiments and time-resolved electrochemical reactions with the *in-situ* characterization of the species via infrared spectroscopy (SEIRA, surface enhanced infrared absorption spectroscopy).[144–146] This method has been shown to be instrumental in the study of metalloenzymes as it can relate the information from "classical" electrochemistry to structural properties. The experimental set-up is illustrated in Figure 9.

The covalent binding and immobilization of the protein on the SEIRA-active gold-coated electrode (working electrode) is achieved by the formation of cysteamine self-assembled monolayers on the thin gold film,[88,147] to avoid direct contact with the metal surface. Figure 9 shows a cyclic voltammogram of the immobilised *D. vulgaris* MF hydrogenase recorded under H_2 atmosphere at pH 5.5. This shows the catalytic current (H_2 oxidation current) as the potential is swept and the enzyme interconverts between active and inactive states. An important parameter in this plot is the so-called "switch potential", E_{sw}, a phenomenological parameter that is related with the onset of catalytic activity (inflection point of catalytic current ascent). This value for *D. vulgaris* MF is -33 mV at pH 5.5 and is in the range of the values reported for other oxygen-sensitive hydrogenases[148] such as *A. vinosum* (-40 mV pH 5.9). At low potentials a region of negative current observed corresponds to H^+ reduction (H_2 evolution). Similar to other standard [NiFe] hydrogenases its magnitude is lower compared to [FeFe] hydrogenases that are more biased towards H_2 production.

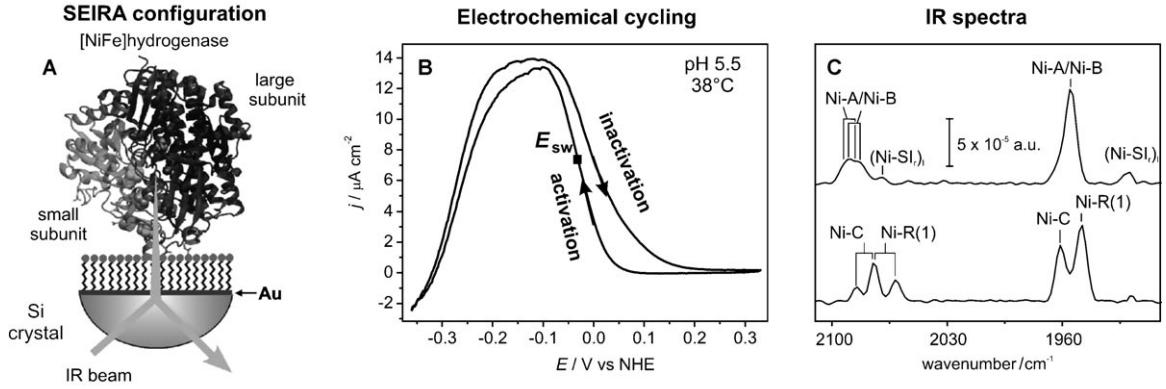

Figure 9. SEIRA setup: A) A thin Au film is formed on the flat surface of a Si semicylindrical crystal for the surface enhanced infrared measurements in a Kretschmann-ATR configuration. The biocompatible immobilisation of the protein is achieved by the formation of cysteamine ($HSCH_2CH_2NH_2$) self-assembled monolayers (SAMs) on the Au electrode surface. B) The anaerobic inactivation and reactivation of *D. vulgaris* MF immobilized on the Au electrodes chemically modified with a SAM of 6-amino-1-hexanethiol is monitored by CV under H_2 atmosphere. The square shows the point of inflection of the ascending current for the reactivation process (E_{sw}) at −33 mV. Measurements were carried out at 38 °C in 50 mM acetate buffer at pH 5.5, scan rate 1 mV s^{-1}. Arrows indicate the scan direction. C) SEIRA spectra of the as-isolated *D. vulgaris* MF enzyme (top) and of H_2-reduced enzyme (~5 h under H_2) (bottom). Experimental conditions: 39 °C, pH 5.5.

The SEIRA spectra obtained for the *D. vulgaris* MF enzyme and the electrochemical investigations yielded essentially identical results with the in-solution FTIR spectroelectrochemistry.[88] This shows that the hydrogenase enzyme remains functionally intact, when wired to an electrode surface. In addition interconversion between redox states can be generated in the presence of a variety of gaseous substances. The SEIRA approach is thus increasingly valuable for the characterisation of hydrogenases as well for their potential use in technological applications such as in biofuel cells.

7. The Catalytic Mechanism of [NiFe] Hydrogenases and the Inhibition of the Enzyme

Based on the spectroscopic and electrochemical data presented in the preceding sections, a large number of intermediates in processes related to the hydrogenase function could be identified and characterized. This knowledge is summarized in the scheme of Figure 10, which is divided into the inactive states, the active states of the catalytic cycle, the CO-inhibited states and the states created by light.

Nickel is the redox active metal ion and thus the functional scheme consists of a number of EPR-active and EPR-silent states. The enzyme cycles between formal Ni^{3+} and Ni^{2+} states as indicated (a formal Ni^{1+} state is only present at cryogenic temperatures under illumination). Ni^{3+} has a d_{z^2} ground state ($S = 1/2$). The EPR-silent states may exist in low ($S = 0$) or high spin states ($S = 1$), a possibility that remains still under discussion. The electronic configuration of the molecular complex is sensitive to several contributions; ligand environment, protonation of the cysteine sulphurs and the geometry. This is shown by DFT calculations in which the singlet and triplet states are close in energy and it thus becomes difficult to conclude with certainty which electronic state is preferred. The iron is not redox active, it is always diamagnetic (low spin Fe^{2+}) coordinated by strong π- and σ- ligands, that is, CO, CN^-.

In the presence of O_2, catalytic ability is lost. The paramagnetic inactive states of the enzyme (Ni-A and Ni-B) have oxo-based ligands bound to the active site bridging Ni and Fe. The Ni-B ("ready") state has a μ-hydroxo bridge accessible to solvent (H/D exchange); this state is quickly activated, a process

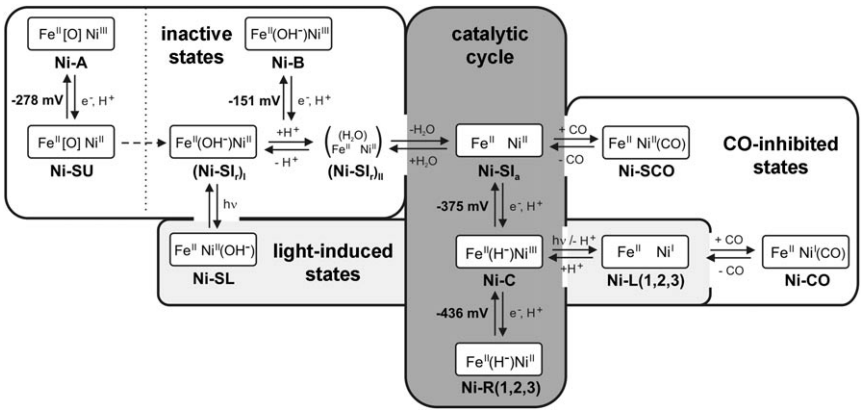

Figure 10. Proposed reaction scheme for the anaerobic [NiFe] hydrogenase from *D. vulgaris* MF based on electrochemical titrations, including both active and inactive intermediates, and CO-inhibited and light-induced states. The formal oxidation states of the Ni and the Fe are given, furthermore the type of bridging ligand that changes identity and its position (in some cases) in the cycle is indicated. In Ni-A and Ni-SU the bridging oxygenic ligand presented by [O] has not been conclusively determined. The midpoint potential for the redox couples are given for pH 7.4, except for the Ni-A to Ni-SU transition, which is given for pH 8.2.

that finally leads to a loss of the bridging ligand in the active Ni-SI_a state of the catalytic cycle. The Ni-A state ("unready") is slowly activated. It is absent in all oxygen-tolerant [NiFe] hydrogenases. A final conclusion on the bridging ligand has not been made. Both states are paramagnetic (Ni^{3+}, $S=1/2$) with the unpaired electron localised mainly on the nickel but have, however, distinct spectroscopic and reactivation kinetic properties.[40,42]

One-electron reduction of Ni-B and Ni-A leads to formation of the EPR-silent (Ni^{2+}) states Ni-SI_r and Ni-SU, respectively. Ni-SI_r exists in two forms that are in an acid-base equilibrium; the $(Ni\text{-}SI_r)_I$ and the more protonated $(Ni\text{-}SI_r)_{II}$, both of which are catalytically inactive.[41,81] In this process, most likely, the μ-hydroxo bridge is protonated to form a short-lived transient H_2O-bound species, $(Ni\text{-}SI_r)_{II}$, prior to converting to the active Ni-SI_a state. On the other hand, Ni-SU exists in one form only, independent of pH, and allegedly has the same oxo-ligand as Ni-A bound to its active site. It has been suggested to convert to the Ni-SI_r states prior to reactivation[86] of the enzyme.

The physiological states, related to dihydrogen catalysis, are reached when the bridging oxygen-based ligand is completely removed from the active site and Ni-SI_a is formed. These are Ni-SI_a, Ni-C and Ni-R (Figure 10). Ni-SI_a is the most oxidised active intermediate and is EPR-silent (Ni^{2+}). It has an open bridging position and the nickel is thus only 4-coordinated. It is suggested that this state most easily attaches the hydrogen, which is polarised and heterolytically split. The Ni is probably the site of H_2 binding since CO is also attached to this metal and the gas access channel ends close to the nickel—but Fe as the initial site of attachment cannot be completely excluded.

Proton coupled one-electron reduction leads to the catalytic Ni-C state. In this step base-assisted heterolytic cleavage of the H_2 molecule takes place, leaving a hydride ligand (H^-) in the bridging position between Ni and Fe[102,106,107] and an electron is released to the proximal Fe_4S_4 cluster. One of the candidates for the respective base is the terminal Cys546[20,39] that then transfers the proton to Glu34 (*D. vulgaris* numbering). This cysteine residue has a high temperature factor indicating conformational flexibility and a possible involvement in proton transfer. Alternatively the proton could be taken up by another cysteine residue or even by a water molecule loosely bound to the Fe as proposed in another mechanism.[85]

Proton coupled one-electron further reduction of Ni-C leads to the EPR-silent state Ni-R. However, Ni-R can also be formed directly from the Ni-SI_a state after its reaction with H_2 and if all three clusters are already reduced, without the Ni-C as a detectable intermediate. Ni-R is the most reduced state of the enzyme and can exist in three isoelectronic forms that differ in the protonation degree either of the coordinating cysteine residues or of the substrate ligands (e.g. H_2, H^-) bound to the active site.[31,91] All details of the mechanism are not yet available, a fact that has led to several mechanistic proposals[11,31,32,93,94,115]. An interesting alternative to the above discussed scheme has been postulated, in which only the Ni-R and Ni-C states are involved in catalysis, except for other (more reduced) transient species.[92]

Several states of the enzyme are light-sensitive; this can be directly correlated with structural changes of its active site. Whereas the fully oxidised states Ni-B and Ni-A are not light-sensitive,[1] the Ni-SI_r state upon illumination forms a light-induced EPR-silent species denoted as Ni-SL.[84] The underlying process has been related to a structural change involving a displacement of the μ-hydroxo ligand. Illumination at low temperatures also affects the Ni-C state and converts it to a paramagnetic state termed Ni-L, with concomitant loss of the hydride bridge in form of a proton.[102,118] Ni-L is described by a formal Ni^{1+} state, with a mixed $d_{z^2}/d_{x^2-y^2}$ ground state.[123] Several Ni-L forms have been reported, which most likely differ with respect to the location of the proton, after its dissociation from the bridging position.[120] Furthermore, there are reports for light-induced structural changes also in the Ni-R states.[125]

The active enzyme can be inhibited by CO and other gaseous molecules.[126,127,149,150] It has been demonstrated by X-ray crystallographic studies that the externally added carbon monoxide binds terminally to the nickel ion.[29] Two distinct CO-inhibited redox states have been characterised by spectroscopy; a paramagnetic Ni-CO and an EPR-silent Ni-SCO state.[128,129] Both are light sensitive, leading to photodissociation of the extrinsic CO ligand; Ni-CO converts to the same Ni-L state as Ni-C, while Ni-SCO converts to Ni-SI_a,[129,133] see Figure 10. Ni^{3+} does not bind CO and in the other states CO binding is difficult when the bridging ligand is still present. Thus, only 4-coordinated nickel in a low oxidation state, either Ni^{2+} as in Ni-SI_a or Ni^{1+} as in Ni-L, has the affinity to bind carbon monoxide. The Ni-CO bond is not very strong; it can be dissociated with light, by flushing with hydrogen or inert gases and by applying very reducing conditions (below −500 mV).

The issue of inhibition by molecular oxygen is significant and has several consequences, for example, for biotechnological applications. In the case of the [FeFe] hydrogenases, exposure to oxygen leads to an irreversible destruction of the enzyme, a degradation process for which mechanisms have been recently proposed.[151,152] [NiFe] hydrogenases have the advantage that they are less oxygen sensitive, with the O_2 inhibition being often reversible, while there are a few hydrogenases, for example, from Knallgas[43,153] or hyperthermophilic bacteria,[154] which are even oxygen tolerant. These do not show the Ni-A state. In this context, it is interesting that the recently obtained X-ray crystallographic structure of the photosynthetic bacterium *A. vinosum* in the Ni-A state appears to carry a monoatomic bridging ligand, which is compatible with the proposal of a hydroxyl ligand based on the experimental data presented here (Ogata et al., to be submitted). The structural information obtained so far is, however, not giving a clear picture for the slow activation of the Ni-A state.

8. Conclusions and Outlook

This minireview focuses on the current knowledge obtained for the standard [NiFe] hydrogenase from *D. vulgaris* MF, which should be generally valid for all known oxygen-sensitive hydrogenases. Great progress has been made during the last years in the understanding of the intermediate states, the activation,

inhibition as well as the light sensitivity of this enzyme, whereas specific aspects are still to be resolved. Concerning the mechanism, it is still not entirely clear, which of the many spectroscopic states are actually involved in the enzyme's activation/inactivation and catalytic cycle. Is there a function of the Fe in hydrogen polarization and splitting? Which is the base taking part in the catalytic process; a cysteine ligand, a water molecule or another unknown site? Furthermore the possible role of high-spin Ni^{2+} in the mechanism remains to be investigated. The inhibition of the enzyme by O_2 leading to the Ni-A state is also not well understood. Future pulse EPR/ENDOR experiments using $^{17}O_2$ and/or $H_2{}^{17}O$ should help to finally identify the bridging ligand. A reinvestigation of Ni-A in hydrogenase single crystals both by X-ray crystallography and EPR spectroscopy is under way in our group to solve this important question.

Experiments with the aim of combining hydrogenase as a producer of H_2 with photosynthetic proteins that split water and produce O_2 are currently pursued in many laboratories. Pertinent problems are the limited stability of the biological components, the low energy efficiency of photosynthesis and the oxygen sensitivity of most hydrogenases. This process—that is actually performed in nature by certain classes of green algae and cyanobacteria—stimulated researchers to study the mechanisms and details of the molecular and electronic structure of all the components involved, including the hydrogenases. If the essentials of the enzymes involved in the catalysis of hydrogen conversion are better understood—in particular their oxygen sensitivity and high turnover rates—it may be possible to either use the isolated enzymes in biotechnology or to build functional, more stable synthetic analogs. In the present review, proposals are made for the structure of the active site in the various intermediate states of oxygen-sensitive hydrogenases as well as their possible role in catalysis, based on combined spectroscopic and theoretical methods. We believe that this study will be useful for understanding the reactivity of these enzymes with H_2 or inhibitors and their future application in biologically based hydrogen technology.

Acknowledgements

The authors are very grateful to all the past and present members of our group who have contributed to this work and who are cited in the respective references. We would like to thank Patricia Malkowski for the purification of the D. vulgaris MF enzyme. Diego Millo, Ingo Zebger, and Peter Hildebrandt (TU Berlin) are gratefully acknowledged for a fruitful collaboration on the SEIRA experiments. Birgit Deckers is particularly thanked for her help with the graphical artwork. This work was financially supported by the EU/Energy Network project SOLAR-H2 (FP7 contract 212508), BMBF (03SF0318B, 03SF0355C), and by the Max Planck Society.

Keywords: electrochemistry · EPR spectroscopy · hydrogenases · IR spectroscopy · spectroscopic techniques

[1] S. Ogo, *Chem. Commun.* **2009**, *23*, 3317 – 3325.
[2] W. Lubitz, W. Tumas, *Chem. Rev.* **2007**, *107*, 3900 – 3903.
[3] K. A. Vincent, J. A. Cracknell, A. Parkin, F. A. Armstrong, *Dalton Trans.* **2005**, *3*, 3397 – 3403.
[4] M. Stephenson, L. H. Stickland, *Biochem. J.* **1931**, *25*, 205 – 214.
[5] P. M. Vignais, A. Colbeau, *Curr. Issues Mol. Biol.* **2004**, *6*, 159 – 188.
[6] R. Mertens, A. Liese, *Curr. Opin. Biotechnol.* **2004**, *15*, 343 – 348.
[7] F. A. Armstrong, N. A. Belsey, J. A. Cracknell, G. Goldet, A. Parkin, E. Reisner, K. A. Vincent, A. F. Wait, *Chem. Soc. Rev.* **2009**, *38*, 36 – 51.
[8] E. Lojou, X. Luo, M. Brugna, N. Candoni, S. Dementin, M. T. Giudici-Orticoni, *J. Biol. Inorg. Chem.* **2008**, *13*, 1157 – 1167.
[9] W. Lubitz, E. J. Reijerse, J. Messinger, *Energy Environ. Sci.* **2008**, *1*, 15 – 31.
[10] P. M. Vignais, B. Billoud, *Chem. Rev.* **2007**, *107*, 4206 – 4272.
[11] W. Lubitz, E. J. Reijerse, M. van Gastel, *Chem. Rev.* **2007**, *107*, 4331 – 4365.
[12] J. C. Fontecilla-Camps, A. Volbeda, C. Cavazza, Y. Nicolet, *Chem. Rev.* **2007**, *107*, 4273 – 4303.
[13] S. Shima, O. Pilak, S. Vogt, M. Schick, M. S. Stagni, W. Meyer-Klaucke, E. Warkentin, R. K. Thauer, U. Ermler, *Science* **2008**, *321*, 572 – 575.
[14] T. Yagi, K. Kimura, H. Daidoji, F. Sakai, S. Tamura, H. Inokuchi, *J. Biochem.* **1976**, *79*, 661 – 671.
[15] R. K. Thauer, K. Jungermann, K. Decker, *Bacteriol. Rev.* 1**977**, 41, 100 – 180.
[16] Y. Higuchi, M. Kusunoki, Y. Matsuura, N. Yasuoka, M. Kakudo, *J. Mol. Biol.* **1984**, *172*, 109 – 139.
[17] N. Yahata, T. Saitoh, Y. Takayama, K. Ozawa, H. Ogata, Y. Higuchi, H. Akutsu, *Biochemistry* **2006**, *45*, 1653 – 1662.
[18] Y. Higuchi, T. Yagi, N. Yasuoka, *Structure* **1997**, *5*, 1671 – 1680.
[19] C. C. Page, C. C. Moser, X. X. Chen, P. L. Dutton, *Nature* **1999**, *402*, 47 – 52.
[20] S. Dementin, B. Burlat, A. L. De Lacey, A. Pardo, G. Dryanczyk-Perrier, B. Guigliarelli, V. M. Fernandez, M. Rousset, *J. Biol. Chem.* **2004**, *279*, 10508 – 10513.
[21] V. H. Teixeira, C. M. Soares, A. M. Baptista, *Proteins Struct. Funct. Bioinf.* **2008**, *70*, 1010.
[22] I. Fdez Galvan, A. Volbeda, J. C. Fontecilla-Camps, M. J. Field, *Proteins* **2008**, *73*, 195 – 203.
[23] A. Volbeda, M. H. Charon, C. Piras, E. C. Hatchikian, M. Frey, J. C. Fontecilla-Camps, *Nature* **1995**, *373*, 580 – 587.
[24] R. P. Happe, W. Roseboom, A. J. Pierik, S. P. J. Albracht, K. A. Bagley, *Nature* **1997**, *385*, 126 – 126.
[25] A. J. Pierik, W. Roseboom, R. P. Happe, K. A. Bagley, S. P. J. Albracht, *J. Biol. Chem.* **1999**, *274*, 3331 – 3337.
[26] A. J. Pierik, M. Hulstein, W. R. Hagen, S. P. J. Albracht, *Eur. J. Biochem.* **1998**, *258*, 572 – 578.
[27] F. Dole, A. Fournel, V. Magro, E. C. Hatchikian, P. Bertrand, B. Guigliarelli, *Biochemistry* **1997**, *36*, 7847 – 7854.
[28] O. Lenz, I. Zebger, J. Hamann, P. Hildebrandt, B. Friedrich, *FEBS Lett.* **2007**, *581*, 3322 – 3326.
[29] H. Ogata, Y. Mizoguchi, N. Mizuno, K. Miki, S. Adachi, N. Yasuoka, T. Yagi, O. Yamauchi, S. Hirota, Y. Higuchi, *J. Am. Chem. Soc.* **2002**, *124*, 11628 – 11635.
[30] Y. Montet, P. Amara, A. Volbeda, X. Vernede, E. C. Hatchikian, M. J. Field, M. Frey, J. C. Fontecilla-Camps, *Nat. Struct. Biol.* **1997**, *4*, 523 – 526.
[31] H. Ogata, W. Lubitz, Y. Higuchi, *Dalton Trans.* **2009**, *37*, 7577 – 7587.
[32] J. C. Fontecilla-Camps, P. Amara, C. Cavazza, Y. Nicolet, A. Volbeda, *Nature* **2009**, *460*, 814 – 822.
[33] Y. Higuchi, T. Yagi, *Biochem. Biophys. Res. Commun.* **1999**, *255*, 295 – 299.
[34] B. H. Huynh, D. S. Patil, I. Moura, M. Teixeira, J. J. G. Moura, D. V. Dervartanian, M. H. Czechowski, B. C. Prickril, H. D. Peck, J. Le Gall, *J. Biol. Chem.* **1987**, *262*, 795 – 800.
[35] C. Bagyinka, J. P. Whitehead, M. J. Maroney, *J. Am. Chem. Soc.* **1993**, *115*, 3576 – 3585.
[36] Z. J. Gu, J. Dong, C. B. Allan, S. B. Choudhury, R. Franco, J. J. G. Moura, J. Le Gall, A. E. Przybyla, W. Roseboom, S. P. J. Albracht, M. J. Axley, R. A. Scott, M. J. Maroney, *J. Am. Chem. Soc.* **1996**, *118*, 11155 – 11165.
[37] H. Wu, M. B. Hall, *C. R. Chim.* **2008**, *11*, 790 – 804.
[38] M. Stein, W. Lubitz, *Curr. Opin. Chem. Biol.* **2002**, *6*, 243 – 249.

[39] M. Bruschi, G. Zampella, P. Fantucci, L. De Gioia, *Coord. Chem. Rev.* **2005**, *249*, 1620 – 1640.
[40] V. M. Fernandez, E. C. Hatchikian, R. Cammack, *Biochim. Biophys. Acta* **1985**, *832*, 69 – 79.
[41] S. Kurkin, S. J. George, R. N. F. Thorneley, S. P. J. Albracht, *Biochemistry* **2004**, *43*, 6820.
[42] S. E. Lamle, S. P. J. Albracht, F. A. Armstrong, *J. Am. Chem. Soc.* **2004**, *126*, 14899 – 14909.
[43] M. Saggu, I. Zebger, M. Ludwig, O. Lenz, B. Friedrich, P. Hildebrandt, F. Lendzian, *J. Biol. Chem.* **2009**, *284*, 16264 – 16276.
[44] M. Saggu, C. Teutloff, M. Ludwig, M. Brecht, M. E. Pandelia, O. Lenz, B. Friedrich, W. Lubitz, P. Hildebrandt, F. Lendzian, R. Bittl, *Phys. Chem. Chem. Phys.* **2010**, *12*, 2139 – 2148.
[45] S. P. J. Albracht, *Biochim. Biophys. Acta Bioenerg.* **1994**, 1188, 167 – 204.
[46] J. J. G. Moura, M. Teixeira, I. Moura, J. Le Gall, *The Bioinorganic Chemistry of Nickel*, (Ed.: J. R. J. Lancaster), Wiley & Sons, **1988**, p. 191.
[47] C. Gessner, O. Trofanchuk, K. Kawagoe, Y. Higuchi, N. Yasuoka, W. Lubitz, *Chem. Phys. Lett.* **1996**, *256*, 518 – 524.
[48] O. Trofanchuk, M. Stein, C. Gessner, F. Lendzian, Y. Higuchi, W. Lubitz, *J. Biol. Inorg. Chem.* **2000**, *5*, 36 – 44.
[49] M. Stein, W. Lubitz, *Phys. Chem. Chem. Phys.* **2001**, *3*, 2668 – 2675.
[50] S. P. J. Albracht, E. G. Graf, R. K. Thauer, *FEBS Lett.* **1982**, *140*, 311 – 313.
[51] S. Foerster, Doctoral Thesis, Technische Universität Berlin (Germany) **2003**.
[52] A. G. Agrawal, Doctoral Thesis, Heinrich-Heine-Universität Düsseldorf (Germany) **2005**.
[53] M. Flores, A. G. Agrawal, M. van Gastel, W. Gärtner, W. Lubitz, *J. Am. Chem. Soc.* **2008**, *130*, 2402 – 2403.
[54] M. Stein, *Doctoral Thesis*, Technische Universität Berlin (Germany) **2001**.
[55] J. E. Huyett, M. Carepo, A. Pamplona, R. Franco, I. Moura, J. J. G. Moura, B. M. Hoffman, *J. Am. Chem. Soc.* **1997**, *119*, 9291 – 9292.
[56] K. K. Surerus, M. Chen, J. W. van der Zwaan, F. M. Rusnak, M. Kolk, E. C. Duin, S. P. J. Albracht, E. Munck, *Biochemistry* **1994**, *33*, 4980 – 4993.
[57] C. L. Fan, M. Teixeira, J. Moura, I. Moura, B. H. Huynh, J. Le Gall, H. D. Peck, B. M. Hoffman, *J. Am. Chem. Soc.* **1991**, *113*, 20 – 24.
[58] J. W. van der Zwaan, J. M. C. C. Coremans, E. C. M. Bouwens, S. P. J. Albracht, *Biochim. Biophys. Acta* **1990**, *1041*, 101 – 110.
[59] M. Carepo, D. L. Tierney, C. D. Brondino, T. C. Yang, A. Pamplona, J. Telser, I. Moura, J. J. G. Moura, B. M. Hoffman, *J. Am. Chem. Soc.* **2002**, *124*, 281 – 286.
[60] B. Bleijlevens, B. W. Faber, S. P. J. Albracht, *J. Biol. Inorg. Chem.* **2001**, *6*, 763 – 769.
[61] M. van Gastel, C. Fichtner, F. Neese, W. Lubitz. *Biochem. Soc. Trans.* **2005**, *33*, 7 – 11.
[62] M. van Gastel, M. Stein, M. Brecht, O. Schroeder, F. Lendzian, R. Bittl, H. Ogata, Y. Higuchi, W. Lubitz, *J. Biol. Inorg. Chem.* **2006**, *11*, 41 – 51.
[63] H. Ogata, S. Hirota, A. Nakahara, H. Komori, N. Shibata, T. Kato, K. Kano, Y. Higuchi, *Structure* **2005**, *13*, 1635 – 1642.
[64] A. Volbeda, L. Martin, C. Cavazza, M. Matho, B. W. Faber, W. Roseboom, S. P. J. Albracht, E. Garcin, M. Rousset, J. C. Fontecilla-Camps, *J. Biol. Inorg. Chem.* **2005**, *10*, 239 – 249.
[65] P. Jayapal, M. Sundararajan, I. H. Hillier, N. A. Burton, *Phys. Chem. Chem. Phys.* **2006**, *8*, 4086 – 4094.
[66] P. E. M. Siegbahn, *C. R. Chim.* **2007**, *10*, 766 – 774.
[67] K. A. Vincent, F. A. Armstrong, *Inorg. Chem.* **2005**, *44*, 798 – 809.
[68] A. Pardo, A. L. De Lacey, V. M. Fernandez, Y. B. Fan, M. B. Hall, *J. Biol. Inorg. Chem.* **2007**, *12*, 751 – 760.
[69] C. A. Grapperhaus, M. Y. Darensbourg, *Acc. Chem. Res.* **1998**, *31*, 451 – 459.
[70] S. E. Lamle, S. P. J. Albracht, F. A. Armstrong, *J. Am. Chem. Soc.* **2005**, *127*, 6595 – 6604.
[71] *S-Centered Radicals*, (Ed.: Z. B. Alfassi), John Wiley & Sons, **1999**.
[72] W. E. Dascent. *Inorg. Energ.* Cambridge University Press, **1982**.
[73] T. B. Liu, B. Li, M. L. Singleton, M. B. Hall, M. Y. Darensbourg, *J. Am. Chem. Soc.* **2009**, *131*, 8296 – 8307.
[74] R. Cammack, D. S. Patil, E. C. Hatchikian, V. M. Fernandez, *Biochim. Biophys. Acta* **1987**, *912*, 98 – 109.
[75] M. Teixeira, I. Moura, A. V. Xavier, J. J. G. Moura, J. Le Gall, D. V. Dervartanian, H. D. Peck, B. H. Huynh, *J. Biol. Chem.* **1989**, *264*, 16435 – 16450.
[76] M. Asso, B. Guigliarelli, T. Yagi, P. Bertrand, *Biochim. Biophys. Acta* **1992**, *1122*, 50 – 56.
[77] M. Brecht, Doctoral Thesis, Technische Universtität Berlin (Germany) **2001**.
[78] J. M. Mouesca, L. Noodleman, D. A. Case, B. Lamotte, *Inorg. Chem.* **1995**, *34*, 4347 – 4359.
[79] C. Elsässer, M. Brecht, R. Bittl, *J. Am. Chem. Soc.* **2002**, *124*, 12606 – 12611.
[80] C. Elsässer, M. Brecht, R. Bittl, *Biochem. Soc. Trans.* **2005**, *33*, 15 – 19.
[81] B. Bleijlevens, F. A. van Broekhuizen, A. L. De Lacey, W. Roseboom, V. M. Fernandez, S. P. J. Albracht, *J. Biol. Inorg. Chem.* **2004**, *9*, 743 – 752.
[82] S. J. George, S. Kurkin, R. N. F. Thorneley, S. P. J. Albracht, *Biochemistry* **2004**, *43*, 6808 – 6819.
[83] A. L. De Lacey, A. Pardo, V. M. Fernandez, S. Dementin, G. Dryanczyk-Perrier, E. C. Hatchikian, M. Rousset, *J. Biol. Inorg. Chem.* **2004**, *9*, 636 – 642.
[84] M. E. Pandelia, H. Ogata, L. J. Currell, M. Flores, W. Lubitz, *J. Biol. Inorg. Chem.* **2009**, *14*, 1227 – 1241.
[85] M. Stein, W. Lubitz, *J. Inorg. Biochem.* **2004**, *98*, 862 – 877.
[86] A. L. De Lacey, E. C. Hatchikian, A. Volbeda, M. Frey, J. C. Fontecilla-Camps, V. M. Fernandez, *J. Am. Chem. Soc.* **1997**, *119*, 7181 – 7189.
[87] C. Fichtner, C. Laurich, E. Bothe, W. Lubitz, *Biochemistry* **2006**, *45*, 9706 – 9716.
[88] D. Millo, M. E. Pandelia, T. Utesch, N. Wisitruangsakul, M. A. Mroginski, W. Lubitz, P. Hildebrandt, I. Zebger, *J. Phys. Chem. B* **2009**, *113*, 15344 – 15351.
[89] N. K. Menon, H. D. Peck, J. Le Gall, A. E. Przybyla, *J. Bacteriol.* **1987**, *169*, 5401 – 5407.
[90] E. Garcin, X. Vernede, E. C. Hatchikian, A. Volbeda, M. Frey, J. C. Fontecilla-Camps, *Structure* **1999**, *7*, 557 – 566.
[91] A. L. De Lacey, V. M. Fernandez, M. Rousset, R. Cammack, *Chem. Rev.* **2007**, *107*, 4304 – 4330.
[92] A. Volbeda, J. C. Fontecilla-Camps, *Bioorganomet. Chem.* **2006**, *17*, 57 – 82.
[93] A. Volbeda, J. C. Fontecilla-Camps, *Dalton Trans.* **2003**, *21*, 4030 – 4038.
[94] A. Pardo, A. L. De Lacey, V. M. Fernandez, H. J. Fan, Y. B. Fan, M. B. Hall, *J. Biol. Inorg. Chem.* **2006**, *11*, 286 – 306.
[95] H. Wang, D. S. Patil, C. Y. Ralston, C. Bryant, S. P. Cramer, *J. Electron Spectroscopy and Related Phenomena* **2001**, *114*, 865 – 871.
[96] S. Q. Niu, L. M. Thomson, M. B. Hall, *J. Am. Chem. Soc.* **1999**, *121*, 4000 – 4007.
[97] S. H. Li, M. B. Hall, *Inorg. Chem.* **2001**, *40*, 18 – 24.
[98] P. Jayapal, M. Sundararajan, I. H. Hillier, N. A. Burton, *Phys. Chem. Chem. Phys.* **2008**, *10*, 4249 – 4257.
[99] Y. Higuchi, H. Ogata, K. Miki, N. Yasuoka, T. Yagi, *Structure* **1999**, *7*, 549 – 556.
[100] S. Foerster, M. Stein, M. Brecht, H. Ogata, Y. Higuchi, W. Lubitz, *J. Am. Chem. Soc.* **2003**, *125*, 83 – 93.
[101] A. Chapman, R. Cammack, C. E. Hatchikian, J. McCracken, J. Peisach, *FEBS Lett.* **1988**, *242*, 134 – 138.
[102] J. P. Whitehead, R. J. Gurbiel, C. Bagyinka, B. M. Hoffman, M. J. Maroney, *J. Am. Chem. Soc.* **1993**, *115*, 5629 – 5635.
[103] A. Müller, E. C. Hatchikian, J. Hüttermann, R. Kappl, R. Cammack, *J. Inorg. Biochem.* **1999**, *74*, 240 – 240.
[104] M. Pavlov, P. E. M. Siegbahn, M. R. A. Blomberg, R. H. Crabtree, *J. Am. Chem. Soc.* **1998**, *120*, 548 – 555.
[105] M. Stein, W. Lubitz, *Phys. Chem. Chem. Phys.* **2001**, *3*, 5115 – 5120.
[106] M. Brecht, M. van Gastel, T. Buhrke, B. Friedrich, W. Lubitz, *J. Am. Chem. Soc.* **2003**, *125*, 13075 – 13083.
[107] S. Foerster, M. van Gastel, M. Brecht, W. Lubitz, *J. Biol. Inorg. Chem.* **2005**, *10*, 51 – 62.
[108] M. B. Hall, S. Q. Niu, L. Thomson, *J. Inorg. Biochem.* **1999**, *74*, 152 – 152.
[109] B. Guigliarelli, C. More, A. Fournel, M. Asso, E. C. Hatchikian, R. Williams, R. Cammack, P. Bertrand, *Biochemistry* **1995**, *34*, 4781 – 4790.
[110] O. Trofanchuk, Doctoral Thesis, Technische Universität Berlin (Germany) **2001**.
[111] L. M. Roberts, P. A. Lindahl, *Biochemistry* **1994**, *33*, 14339 – 14350.
[112] M. Y. Darensbourg, E. J. Lyon, J. J. Smee, *Coord. Chem. Rev.* **2000**, *206*, 533 – 561.
[113] L. De Gioia, P. Fantucci, B. Guigliarelli, P. Bertrand, *Inorg. Chem.* **1999**, *38*, 2658 – 2662.

[114] L. M. Roberts, P. A. Lindahl, *J. Am. Chem. Soc.* **1995**, *117*, 2565 – 2572.
[115] S. O. Lill, P. E. Siegbahn, *Biochemistry* **2009**, *48*, 1056 – 1066.
[116] T. Matsumoto, B. Kure, S. Ogo, *Chem. Lett.* **2008**, *37*, 970 – 971.
[117] S. Ogo, R. Kabe, K. Uehara, B. Kure, T. Nishimura, S. C. Menon, R. Harada, S. Fukuzumi, Y. Higuchi, T. Ohhara, T. Tamada, R. Kuroki, *Science* **2007**, *316*, 585 – 587.
[118] J. W. van der Zwaan, S. P. J. Albracht, R. D. Fontijn, E. C. Slater, *FEBS Lett.* **1985**, *179*, 271 – 277.
[119] M. Medina, R. Williams, R. Cammack, E. C. Hatchikian, *J. Chem. Soc. Faraday Trans.* **1994**, *90*, 2921 – 2924.
[120] M. Medina, E. C. Hatchikian, R. Cammack, *Biochim. Biophys. Acta Bioenerg.* **1996**, *1275*, 227 – 236.
[121] F. Dole, M. Medina, C. More, R. Cammack, P. Bertrand, B. Guigliarelli, *Biochemistry* **1996**, *35*, 16399 – 16406.
[122] G. Davidson, S. B. Choudhury, Z. J. Gu, K. Bose, W. Roseboom, S. P. J. Albracht, M. J. Maroney, *Biochemistry* **2000**, *39*, 7468 – 7479.
[123] M. van Gastel, W. Lubitz. *High Resolution EPR: Applications to Metalloenzymes and Metals in Medicine*, Springer, Dordrecht, **2009**, 441 – 470.
[124] P. Kellers, M. E. Pandelia, L. J. Currell, H. Görner, W. Lubitz, *Phys. Chem. Chem. Phys.* **2009**, *11*, 8680 – 8683.
[125] Bagley, K. A. personal communication. 2009.
[126] L. Purec, A. I. Krasna, D. Rittenberg, *Biochemistry* **1962**, *1*, 270 – 275.
[127] G. Fauque, Y. Berlier, E. S. Choi, H. D. Peck, J. Le Gall, P. A. Lespinat, *Biochem. Soc. Trans.* **1987**, *15*, 1050 – 1051.
[128] A. L. De Lacey, C. Stadler, V. M. Fernandez, E. C. Hatchikian, H. J. Fan, S. H. Li, M. B. Hall, *J. Biol. Inorg. Chem.***2002**, *7*, 318 – 326.
[129] M. E. Pandelia, H. Ogata, L. J. Currell, M. Flores, W. Lubitz, *Biochim. Biophys. Acta Bioenerg.* **2010**, *1797*, 304 – 313.
[130] R. P. Happe, W. Roseboom, S. P. J. Albracht, *Eur. J. Biochem.* **1999**, *259*, 602 – 608.
[131] O. Sorgenfrei, A. Klein, S. P. J. Albracht, *FEBS Lett.* **1993**, *332*, 291 – 297.
[132] M. Stein, E. van Lenthe, E. J. Baerends, W. Lubitz, *J. Am. Chem. Soc.* **2001**, *123*, 5839 – 5840.
[133] K. A. Bagley, E. C. Duin, W. Roseboom, S. P. J. Albracht, W. H. Woodruff, *Biochemistry* **1995**, *34*, 5527 – 5535.
[134] H. Frauenfelder, S. G. Sligar, P. G. Wolynes, *Science* **1991**, *254*, 1598 – 1603.
[135] M. Brecht, M. Stein, O. Trofanchuk, F. Lendzian, Y. Higuchi, W. Lubitz in *Magnetic Resonance and Related Phenomena, Vol. II* (Eds: Ziessow D., Lendzian F., Lubitz W.) Technische Universität, Berlin, **1998**, pp. 818 – 819.
[136] T. Buhrke, M. Brecht, W. Lubitz, B. Friedrich, *J. Biol. Inorg. Chem.* **2002**, *7*, 897 – 908.
[137] A. G. Agrawal, M. van Gastel, W. Gärtner, W. Lubitz, *J. Phys. Chem. B* **2006**, *110*, 8142 – 8150.
[138] M. C. Machczynski, H. B. Gray, J. H. Richards, *J. Inorg. Biochem.* **2002**, *88*, 375 – 380.
[139] A. L. De Lacey, E. Santamaria, E. C. Hatchikian, V. M. Fernandez, *Biochim. Biophys. Acta Bioenerg.* **2000**, *1481*, 371 – 380.
[140] C. Léger, P. Bertrand, *Chem. Rev.* **2008**, *108*, 2379 – 2438.
[141] K. A. Vincent, N. A. Belsey, W. Lubitz, F. A. Armstrong, *J. Am. Chem. Soc.* **2006**, *128*, 7448 – 7449.
[142] C. Léger, S. Dementin, P. Bertrand, M. Rousset, B. Guigliarelli, *J. Am. Chem. Soc.* **2004**, *126*, 12 162 – 12 172.
[143] H. R. Pershad, J. L. C. Duff, H. A. Heering, E. C. Duin, S. P. J. Albracht, F. A. Armstrong, *Biochemistry* **1999**, *38*, 8992 – 8999.
[144] M. Osawa, *Bull. Chem. Soc. Jpn.* **1997**, *70*, 2861 – 2880.
[145] K. Ataka, J. Heberle, *Anal. Bioanal. Chem.* **2007**, *388*, 47 – 54.
[146] N. Wisitruangsakul, O. Lenz, M. Ludwig, B. Friedrich, F. Lendzian, P. Hildebrandt, I. Zebger, *Angew. Chem.* **2009**, *121*, 621 – 623; *Angew. Chem. Int. Ed.* **2009**, *48*, 611 – 613.
[147] O. Ruediger, J. M. Abad, E. C. Hatchikian, V. M. Fernandez, A. L. De Lacey, *J. Am. Chem. Soc.* **2005**, *127*, 16 008 – 16 009.
[148] A. K. Jones, S. E. Lamle, H. R. Pershad, K. A. Vincent, S. P. J. Albracht, F. A. Armstrong, *J. Am. Chem. Soc.* **2003**, *125*, 8505 – 8514.
[149] A. I. Krasna, D. Rittenberg, *Proc. Natl. Acad. Sci. USA* **1954**, *40*, 225 – 227.
[150] N. A. Zorin, B. Dimon, J. Gagnon, J. Gaillard, P. Carrier, P. M. Vignais, *Eur. J. Biochem.* **1996**, *241*, 675 – 681.
[151] M. T. Stiebritz, M. Reiher, *Inorg. Chem.* **2009**, *48*, 7127 – 7140.
[152] S. T. Stripp, G. Goldet, C. Brandmayr, O. Sanganas, K. A. Vincent, M. Haumann, F. A. Armstrong, T. Happe, *Proc. Natl. Acad. Sci. USA* **2009**, *106*, 17331 – 17336.
[153] M. Ludwig, J. A. Cracknell, K. A. Vincent, F. A. Armstrong, O. Lenz, *J. Biol. Chem.* **2009**, *284*, 465 – 477.
[154] M. Guiral, P. Tron, V. Belle, C. Aubert, C. Léger, B. Guigliarelli, M. T. Giudici-Orticoni, *Int. J. Hydrogen Energy* **2006**, *31*, 1424 – 1431.

Received: December 4, 2009
Published online on March 18, 2010

CHEMPHYSCHEM

Supporting Information

Intermediates in the Catalytic Cycle of [NiFe] Hydrogenase: Functional Spectroscopy of the Active Site

Maria-Eirini Pandelia, Hideaki Ogata, and Wolfgang Lubitz*[a]

cphc_200900950_sm_miscellaneous_information.pdf

Supplementary Information

Table S1: Experimental g-tensor values for the various paramagnetic states of the [NiFe] hydrogenase from *D. vulgaris* MF hydrogenase.

State	g_x	g_y	g_z
Ni-A	2.32	2.24	2.01
Ni-B	2.33	2.16	2.01
Ni-C	2.20	2.14	2.01
Ni-L	2.30	2.12	2.05
Ni-CO	2.13	2.08	2.02

Table S2: Stretching vibrations of the CO and CN^- ligands for each redox state of the [NiFe] hydrogenase from *D. vulgaris* Miyazaki F at 25 °C (298 K). Values at 100 K are given in parenthesis.

State	IR frequencies , cm^{-1}			
	$\tilde{\nu}_{CO}(Fe)$	$\tilde{\nu}^{asym}{}_{CN}(Fe)$	$\tilde{\nu}^{sym}{}_{CN}(Fe)$	$\tilde{\nu}_{CO}(Ni)$
Ni-A	1956	2085	2094	-
Ni-B	1955	2081	2090	-
Ni-SU	1958	2089	2100	-
$(Ni\text{-}SI_r)_I$	1921	2061	2070	-
$(Ni\text{-}SI_r)_{II}$	1943	2074	2086	-
$Ni\text{-}SI_a$	1943	2074	2086	-
	(1946)	(2077)	(2090)	(-)
Ni-C	1961	2074	2085	-
$Ni\text{-}R_I$	1948	2061	2074	-
$Ni\text{-}R_{II}$	1932	2052	2066	-
$Ni\text{-}SCO_{1941}$	1941	2071	2084	2056
	(1941)	(2072)	(2086)	(2061)
$Ni\text{-}SCO_{red}$	1939	2070	2083	2054
	(1940)	(2071)	(2086)	(2060)